Simple and Robust Study of Backbone Dynamics of Crystalline Proteins Employing H-1-N-15 Dipolar Coupling Dispersion

Piotr Paluch, Tomasz Pawlak, Karol Lawniczak, Julien Trebosc, Olivier Lafon, Jean-Paul Amoureux, Marek J Potrzebowski

Simple and robust study of backbone dynamics of crystalline proteins employing ^{1}H-^{15}N dipolar coupling dispersion

Piotr Paluch,[†§*] Tomasz Pawlak,[†] Karol Ławniczak,[‡] Julien Trébosc,[‖] Olivier Lafon,[‖] Jean-Paul Amoureux,[‖⊥] and Marek J. Potrzebowski[†*]

[†] Centre of Molecular and Macromolecular Studies, Polish Academy of Sciences, Sienkiewicza 112, PL-90363 Łódź, Poland

[‡] Department of Theoretical Physics, Faculty of Physics and Applied Informatics, University of Łódź, Pomorska 149/153, PL-90236 Łódź, Poland

[‖] Univ. Lille, UMR 8181, UCCS: Unit of Catalysis and Chemistry of Solids, F-59000 Lille, France

[⊥] Bruker France, 34 rue de l'Industrie, F-67166 Wissembourg, France

Abstract

We report a new solid state multi-dimensional NMR approach based on the CPVC pulse sequence (P. Paluch, T. Pawlak, J.-P. Amoureux, M.J. Potrzebowski, *J. Magn. Reson*. 233 (2013) 56), with ^{1}H inverse-detection and very fast magic angle spinning (ν_R = 60 kHz), dedicated to the measurement of local molecular motions of ^{1}H-^{15}N vectors. The introduced 3D experiments, ^{1}H-^{15}N-^{1}H and hCA(N)H, are particularly useful for the study of molecular dynamics of proteins and other complex structures. The applicability and power of this methodology has been revealed by employing as a model sample the GB-1 small protein doped with $Na_2CuEDTA$. The results clearly prove that the dispersion of ^{1}H-^{15}N dipolar coupling constants well correlates with higher order structure of the protein. Our approach complements the conventional studies and offers a fast and reasonably simple method.

INTRODUCTION

To understand in detail the biological functions of proteins, knowledge of their dynamics is crucial. Indeed, it is well-known that protein motions occurring on the pico- to millisecond time scales play important functional roles,[1] and that dynamics modulates the interactions between physiological partners.[2] A large amount of experimental and computational methods have been developed and applied to study protein dynamics at different time and length scales. As an example fluorescence techniques,[3] atomic force microscopy,[4] and optical or magnetic tweezers,[5] usually analyze dynamics on length scales of a few tens of Å and time scales longer than milliseconds. Nuclear magnetic resonance (NMR),[6] neutron scattering,[7] and Molecular Dynamics (MD) simulations,[8] are among the techniques that allow direct analyses of atomic motions from pico-seconds to seconds.

The unique feature of NMR spectroscopy is the possibility to analyze the dynamics of biomolecules at atomic resolution both in the liquid and solid states. Study of proteins in solids seems particularly attractive because the overall tumbling, which interferes in the liquid phase with the small local motions is eliminated. Several NMR analyses of dynamics, such as measurements of relaxation rates,[9,10] CPMG or $T_{1\rho}$ relaxation dispersion profiles,[11,12,13] pioneering high resolution T_1 relaxation dispersion[14] and magnetization or hydrogen exchange rates,[15] can be carried out in liquid and solid states. Solid-state NMR (ssNMR) methodologies mostly exploit the analysis of anisotropic tensorial interactions, such as dipolar coupling[16,17,18,19,20,21,22,23] and CSA (chemical shift anisotropy).[24,25,26] However, these anisotropic interactions are averaged to zero by a fast sample spinning at the magic angle (MAS) in terms of the first order Average Hamiltonian Theory (AHT). To date, a large number of techniques have been developed to reintroduce these anisotropic interactions with pulse sequences that are often based on symmetry rules introduced by Levitt.[27,28] These sequences are called CN^{ν}_{n} and RN^{ν}_{n} where the symbols N, n, and ν are small symmetry

integer numbers that depend on the rotation properties of the spin angular moment during the rotor-synchronized train of radio-frequency (rf) pulses. In this strategy the relationship between spins, space, rotation and rf-pulses is used to amplify the desired and suppress the unwanted interactions. As an example, the recently published RN-CSA symmetry schemes are suitable for CSA recoupling at fast spinning speeds ($\nu_R \geq 40$ kHz).[29] Other important sequences designed to measure dipolar couplings are based on REDOR[18,19] T-MREV[20,21] and CPPI[22] approaches.

In this paper, we report a method named cross-polarization with variable-contact (CPVC),[30] which is based on a different philosophy and which allows for a simple, accurate and robust way to analyze local molecular motions in the solid state *via* the analysis of heteronuclear dipolar couplings. The main advantage of this method is that it offers a three times larger scaling factor compared to sequences based on CN^{ν}_{n} or RN^{ν}_{n} schemes. Moreover, the application of these two symmetry based recoupling schemes is problematic under ultra-fast MAS ($\nu_R \geq 60$ kHz) due to rf-field limitations. Another motivation to design CPVC approaches is the fact that REDOR type of experiments may be difficult to use in the case of ultra-fast MAS due to finite pulse durations. On the other hand, ultra-fast MAS is more and more frequently used in ssNMR, and presently probe-heads allowing sample spinning rates over 110 kHz are commercially available.[31,32]

The power of this CPVC approach is demonstrated here with a GB-1 protein. We employed a sample doped with a paramagnetic $Na_2CuEDTA$ salt (called GB-1_{Cu}) to reduce the relaxation delay between two accumulations in order to save experimental time, a procedure frequently used, for which a detailed analysis has been provided by Linser et. al.[33] Since one of the purposes of our work is to develop proton-detected sequences to analyze the H-N dipolar couplings, we have used a ^{2}H, ^{13}C, ^{15}N labeled GB-1_{Cu} sample with back-exchanged labile (N-H) protons. Indeed, the ^{2}H labeling greatly increases the spectral

resolution in the ^{1}H domain, especially at fast MAS. However, it must be mentioned that the ^{1}H linewidths still decrease when the spinning speed increases over ν_R = 110 kHz.[34] GB-1_{Cu} is often used to develop and test new methodological approaches, e.g. by Ishii's group.[35] Nevertheless, it is rather surprising that a full site specific assignment for this GB-1_{Cu} sample had not yet been published when we started this project.

METHODOLOGY

NMR measurement

The $^{2}H/^{13}C/^{15}N$ GB-1_{Cu} sample with back-exchanged labile (N-H) protons was purchased as an already filled 1.3 mm rotor from Giotto-Biototech/Cortecnet and was used as received. All experiments were performed at 14.1 T on a Bruker Avance III 600 spectrometer equipped with a 1.3 mm $^{1}H/^{13}C/^{15}N$ CPMAS probe-head operated at frequencies of: 600.1, 150.9 and 60.8 MHz for ^{1}H, ^{13}C and ^{15}N, respectively. In all cases, the sample was spun at ν_R = 60 kHz and the recycling delay was equal to τ_{RD} = 200 ms. For assignments, we used series of ^{1}H-detected experiments, either 2D (hNH) or 3D (hCONH, hCANH, hcaCOcaNH, hcoCAcoNH, hcaCBcaNH, hcaCBcacoNH) as described by Pintacuda *et al.*[36,37] All experiments started from the proton, which is indicated with the h at the beginning of their names, following Pintacuda's convention.[19] For the benefit of non-experts in ssNMR of proteins, these sequences are shortly described in the ESI. Moreover, we also collected two ^{13}C-detected 2D correlations (hNCA and hNCO) based on the double CP scheme. Detailed information about rf-fields, number of points, spectral widths, number of scans, etc. are presented in ESI. Spectra were processed using TopSpin 3.1. In case CPVC experiment RF were near to 20 and 40 for ^{1}H and ^{15}N respectively, actual power were precisely calibrated on each experiments. In the case of 3D CPVC experiments, after two standard FTs along the two chemical shift dimensions, the imaginary part of the spectrum was set to zero with a Python script calling the "dd" Unix commend, and then a real FT was performed along the dipolar dimension, without

any apodization. To remove the strong peak at the center of the dipolar spectrum, the 'qfil' baseline correction implemented in TopSpin was used. For analyses of 2D and 3D spectra, we used Sparky 3.115 with NMRFAM-Sparky extensions. Strip plots from 3D datasets were prepared using NMR Glue.[38,39]

RESULTS AND DISCUSSION

Assigning GB-1$_{Cu}$

The literature reporting structural studies of ^{13}C and/or ^{15}N labeled GB-1 proteins by means of ssNMR is very extensive. A survey of the published works clearly shows that most of the results come from the Rienstra's group.[40] In the cited papers, authors have employed different multi-dimensional ssNMR techniques for the assignments of GB-1, including 2D ^{13}C-^{13}C DARR/SPC-5, 2D/3D N(CO)CX and N(CA)CX, and 3D CONCA. The same group has shown the first application of the 4D CANCOCX sequence for the chemical shifts assignment and thus performed a more accurate structural analysis of GB-1.[41] In these articles, the $^{13}C/^{15}N$ isotopes were directly detected. To the best of our knowledge, the first approach utilizing the inverse mode *via* ^{1}H detection for the assignment of GB-1 (and other proteins) in the solid state has been presented by Zhou *et al.*,[42,43] and this methodology was tested with ν_R = 40 kHz. With current hardware developments, the reduction of rotor diameters allows for an increase of the spinning rate up to ν_R = 150 kHz presently, and this inverse detection approach has found a large number of spectacular applications. Recent articles of Pintacuda *et al.*,[36] Shanda *et al.*,[44] and others,[45,46] provide straightforward evidences showing the power of ^{1}H inverse detection based on very fast MAS techniques. As a consequence, novel spectral editing methods, which permit drastic spectral simplifications, have been recently proposed.[35]

Despite the large number of papers published so far, the structural refinement of our GB-1_{Cu} crystalline sample is not trivial, even if the assignment of signals is unambiguous. The first problem is related to the polymorphism of GB-1. Indeed, it is well known that this protein exists at least in 5 different polymorphic forms, which are characterized by slightly different chemical shifts.[47] It should be noted that other proteins exhibit such polymorphism, e.g. ubiquitin,[48] and thus this problem is quite general. Moreover, differences in experimental chemical shifts can be caused by a tiny miss-calibration, use of different external standards (*e.g.* TSP vs. glycine) or other factors including substitution of protons by deuterons. Indeed, deuteration may affect the ^{13}C chemical shifts, changing their values in the range of 0.2-1.5 ppm for each directly bonded position due to secondary $^{1}H/^{2}H$ isotopic effects.[49] However, such changes are much lower for adjacent $^{2}H/^{13}C$ pairs and they rarely exceed 0.1 ppm. Additionally, we used a $^{2}H/^{13}C/^{15}N$ enriched protein doped with paramagnetic additives in order to reduce the relaxation time. Such an approach, called PACC (Paramagnetic-Assisted Condensed data Collection)[50] has found a large number of impressive applications in structural studies of crystalline proteins. When using PACC, ultrafast MAS and Non-Uniform Sampling, it has recently been shown that ^{1}H inverse detection ^{1}H-^{15}N HETCORs can be recorded as fast as in 9 seconds on GB-1_{Cu}.[51] However, it must be stressed that paramagnetic additives can disturb all chemical shifts due to the pseudo-contact shift (PCS),[52] or the direct Fermi contact shift (FCS), and that the changes strongly depend on the distance and angular position between the observed nuclei and the paramagnetic center. In the case of Cu^{2+}, the PCS could be neglected due to the isotropic magnetic susceptibility tensor. On the contrary, the FCS could be observed even in such case, in particular for the closest nuclei to the paramagnetic centers. Such FCS interaction should not be neglected in general, as it can lead to significant chemical shift changes due to the interaction between the protein and Cu^{2+}. Following these difficulties (polymorphism, deuteration and interaction with the paramagnetic

center), and to be sure of our refinement, we decided to carry out a *de novo* assignment of signals for our GB-1_{Cu} sample.

Our assignment strategy is very similar to the scheme proposed by Bax and co-workers for structural analyses of proteins in the liquid state.[53,54,49] In these articles, different variants of 3D HNCA/HN(CO)CA experiments were employed. In our current project, series of 2D (hNH, hNCO, hNCA) and ^{1}H-detected 3D (hCONH, hCANH, hcaCOcaNH, hcoCAcoNH, hcaCBcaNH, hcaCBcacoNH) experiments were carried out.[36] Comparing the liquid and solid-state NMR approaches, it has to be emphasized that for the hCANH experiment performed on condensed matter, only correlations between H(i)-N(i)-Ca(i) are seen, whereas both H(i)-N(i)-Ca(i) and H(i)-N(i)-Ca(i-1) correlations are visible in HNCA experiment in the liquid phase. This is due to the fact that in the liquid state the magnetization is transferred *via* scalar coupling, and that $^{1}J_{NCa}$ and $^{2}J_{NCa}$ have very similar values. In ssNMR experiments, the magnetization is transferred *via* CPMAS, exploiting the dipolar interactions, which are strongly distance dependent, $D \propto r_{ij}^{-3}$, and hence the transfer of magnetization between not directly bonded atoms is very ineffective. It should be noted that J-coupling based protein experiments also exist in ssNMR, and such strategy was proposed e.g. by Rienstra and Mueller. [55] In such cases, both intra- and inter-residual correlations are visible on some of the residues. A more extended description of assignments with a Table giving the chemical shifts is presented in the ESI. 2D spectra and some representative strip plots from 3D spectra are presented in Fig. 1,2 and S14-S18. In addition, structure calculations using CS-ROSETTA and comparison with previous data are also included in the ESI. In addition chemical shift data have deposited in BioMagResBank at reference number 27562.

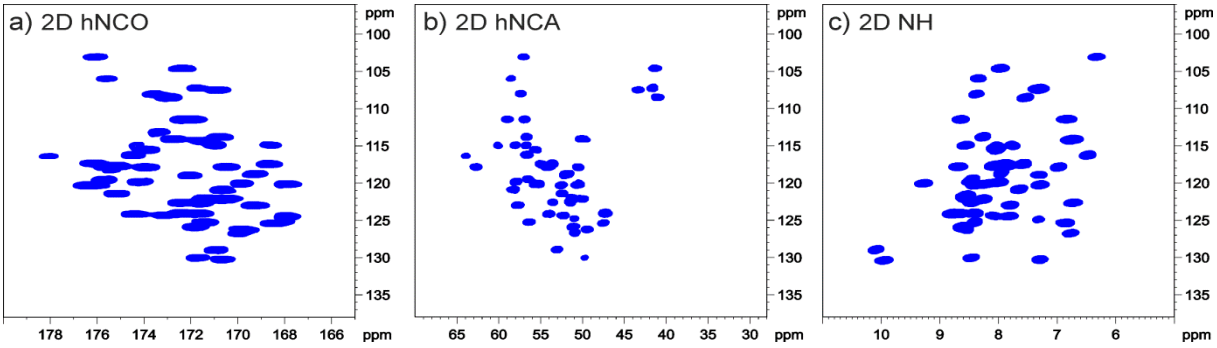

Figure 1. hNCO (a), hNCA (b), hNH (c) 2D spectra for GB-1_{Cu}. Larger size spectra with assignments are presented in ESI.

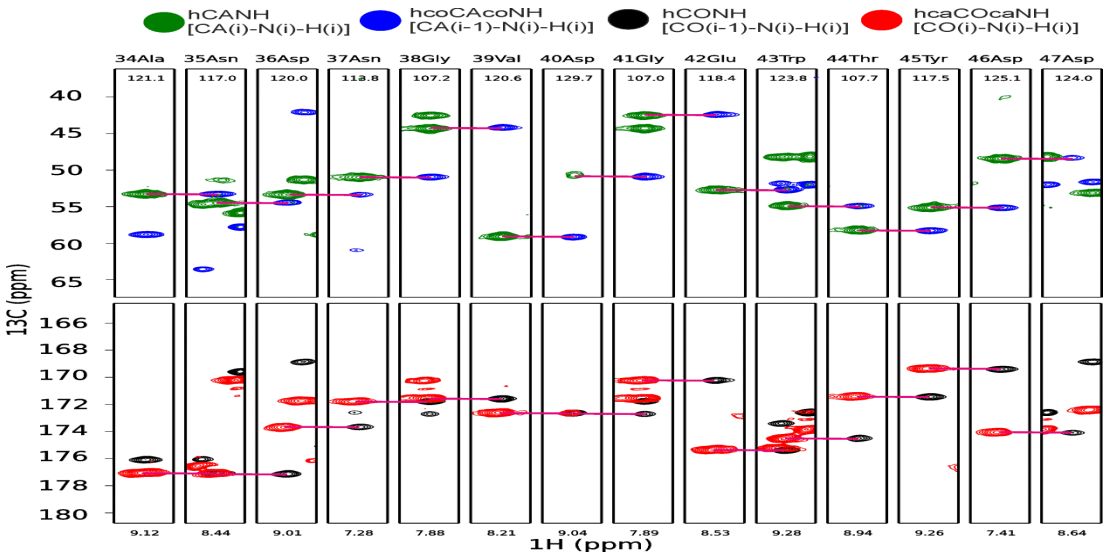

Figure 2. Strip plots from 3D hCANH, hcoCAcoNH, hCONH, hcaCOcaNH for residues from 34Ala to 47Asp. Full sets of strip plots are given in ESI.

Dynamic process analysis

ssNMR is one of the most powerful techniques to study dynamic processes in condensed matter. This ability is related to the very large sensitivity of the various NMR observables to dynamics over large time-scale ranges, and it is possible to observe microscopic motions occurring between pico- to hundreds of seconds. Such methods can be classified into five different groups based on: (i) relaxation (R_1, R_2, $R_{1\rho}$ etc),[56,57,58] (ii) dipolar and (iii) quadrupolar couplings,[59,60] (iv) chemical shift anisotropy,[24] and (v) chemical exchange.[61,62] These methods, which are sensitive to very different time scales, are applicable to small

molecules,[63] polymers,[64] and biomolecules.[65] In the case of biomolecules, relaxation and dipolar coupling-based methods have wider uses.

Quantitative relaxation studies often require either a definition of the model of dynamics or a usage of a model-free approach based on the formalism proposed by Lipari and Szabo.[66,67] In both cases, numerical calculations are required and it is necessary to collect a large amount of high quality spectra to precisely determine the various relaxation parameters. However, these methods allow an accurate determination of the motional timescales, which is not really possible with other methods. Conventional qualitative or semi-quantitative analyses, e.g. by direct comparison of T_2 values, only require the determination of relaxation rates. However, this type of analysis can become problematic when a paramagnetic doping is used. Indeed, in such case the relaxation rates change, and these changes are related to specific interactions of the protein with the paramagnetic center. Therefore, these paramagnetic relaxation changes are not uniform around the whole protein molecule. This strongly complicates the analysis of relaxation data in the case of paramagnetic doping and such data must be treated very carefully. Nevertheless, it should be noted that these paramagnetic relaxation changes should not always be considered as drawbacks, and they can also be used as valuable restrains for structure calculation.[68]

On the contrary, dipolar-based methods usually do not require complicated data treatments, and they often only necessitate collecting a single spectrum. More importantly, the interactions with paramagnetic centers do not change the dipolar couplings, which leads to an easy interpretation of data in the case of the PACC strategy.[50] It is important to remember that the PACC approach decreases by a factor of 5 to 10 the recycling delay with respect to the conventional approach. Therefore, even if we consider that for the dipolar dimension we need more points than for the "relaxation" dimension, the total experiment time is comparable or even lower than with relaxation measurements. Unfortunately, the full information of the time-scales is lost. Indeed, if we consider the two most typical ^{1}H-^{15}N and ^{1}H-^{13}C dipolar couplings for biomolecules, these methods only allow one to know if a process with a time-scale smaller than 10 μs exists or not. Occasionally, some motional models can be proposed from the reduced dipolar tensor parameters. In this article, we use one of these dipolar-based methods for a fast analysis of the backbone dynamics in GB-1_{Cu}. Since the dynamics of the GB-1 protein is well known, with a large number of datasets mostly based on relaxation measurements,[56,69] the purpose of this work is to perform a comparative analysis of CPVC results with the existing data and to demonstrate that our results are in good agreement with

the literature, and at the same time obtained with a methodology easily applicable under very-fast MAS.

Recently, we proposed a new 2D approach, called CPVC (Cross-Polarization with Variable-Contact), to measure the ^{1}H-^{15}N or ^{1}H-^{13}C dipolar couplings.[30] This simple method consists of a controlled $^{1}H \rightarrow {}^{15}N$ or $^{1}H \rightarrow {}^{13}C$ CP transfer under very fast MAS ($\nu_R \geq 60$ kHz). The F2 dimension corresponds to the ^{15}N or ^{13}C chemical shifts (δ_{15N} or δ_{13C}) and the F1 dimension is the $^{1}H \rightarrow {}^{15}N$ or $^{1}H \rightarrow {}^{13}C$ dipolar recoupled spectrum. This spectrum presents two symmetrical narrow peaks, the separation of which is called the dipolar splitting, Δ. The dipolar coupling is described by a second rank tensor with a null trace. When there is no motion, one eigenvalue is equal to $D = \mu_0\gamma_i\gamma_j/4\pi^2r_{ij}^3$ and the two others to -D/2, and hence the dipolar asymmetry parameter is equal to $\eta = 0$. In this case, the dipolar value can directly be determined from the dipolar splitting, $\Delta = D/\sqrt{2}$. When a molecular motion exists, an averaging occurs over the different orientations of the **H-N** or **H-C** vector. This motion leads to a decrease of the D value and an increase of the η parameter in the 0-1 range.[70] The D and η values depend on the amplitude of the motion and on its topology, but they are independent on its time-scale, at least when this motion is fast enough. The CPVC method allows for the measurement of the D and η dipolar coupling parameters, averaged by the molecular motions, but a fitting of the dipolar spectrum may be required to obtain accurate values for these two parameters. We have shown that the $^{1}H \rightarrow {}^{15}N$, $^{1}H \rightarrow {}^{13}C$ or $^{1}H \rightarrow {}^{31}P$ CPVC schemes are very useful in the case of small molecules,[71] or peptides,[72] and we have fully validated their use for quantitative analyses of dynamics with numerical simulations.[73] In addition, we have shown that such analyses can be run in inverse-detected mode ($^{1}H \rightarrow {}^{15}N \rightarrow {}^{1}H$ or $^{1}H \rightarrow {}^{13}C \rightarrow {}^{1}H$ with two CPMAS transfers),[74] and have used this inverse detection to study not only dynamic processes but also hydrogen bonding phenomena.[75] Opella has demonstrated that such an approach is also useful to study the protein backbone dynamics, when it is developed into a 3D inverse-detected experiment for ^{1}H-^{15}N dipolar coupling measurements.[76] Simultaneously, we have proposed another 3D method, called CPVC-RFDR, with ^{13}C detection ($D_{1H\text{-}13C}$-δ_{13C}-δ_{13C}), for dynamics studies of protein side-chains aromatic rings.[77] To the best of our knowledge, it was the first attempt to study such process with atomic resolution.

In the current project, we focused our attention on the backbone dynamics using inverse-detected 3D experiments. In the first part, we used the 3D inverse-detected ^{1}H-^{15}N-^{1}H CPVC method to measure the $D_{1H\text{-}15N}$ values with ^{1}H and ^{15}N chemical shift editing (δ_{15N}-$D_{1H\text{-}15N}$-δ_{1H}). The CPVC sequence is an adaptation to our method modified by inverse-detected

approach described by Pruski.[78,79,80] In our modification, only one change is required: the second CPMAS transfer must be performed with constant rf-fields (Fig. 3).

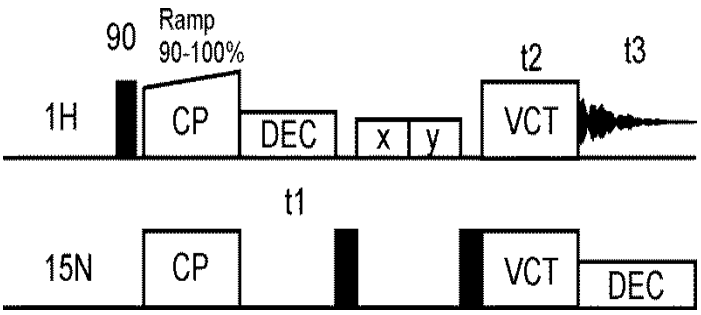

Figure 3. Such an approach has been previously described in a 2D version.[58,59]

This approach allows for an easy determination of the ***H-N*** vectors that have enough mobility to partially average their dipolar interactions. The 2D (δ_{15N}-$D_{1H\text{-}15N}$) projection from the full 3D cube (**Fig. 4**) shows that some residues have lower dipolar splitting values, Δ, and hence lower dipolar couplings. However, it is clear that such simple 2D analysis is not sufficient to precisely determine the dynamics processes for proteins, due to limited resolution along the ^{15}N dimension. Indeed, the F1 dipolar slices may be the sum of several overlapping signals, as shown in **Fig. 4** for δ_{15N} = 105 and 108 ppm.

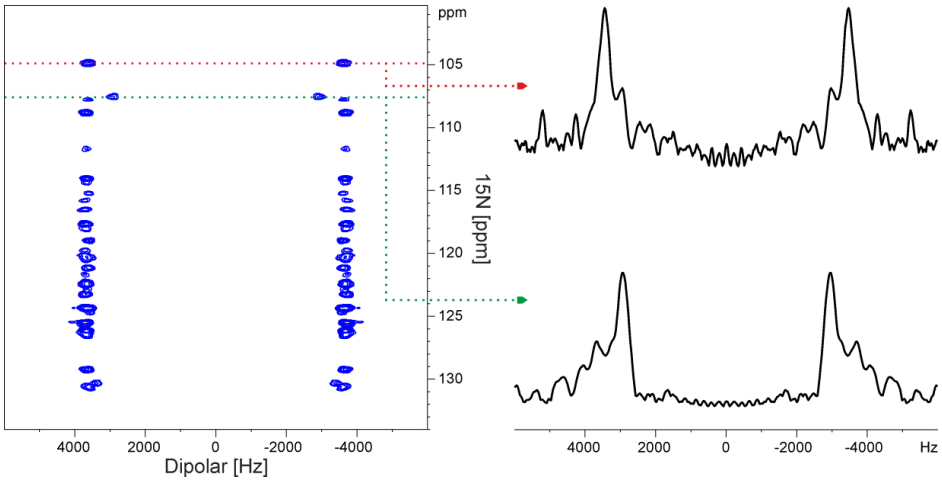

Figure 4. GB-1_{Cu}: δ_{15N}-$D_{1H\text{-}15N}$ projection from the ^{1}H-^{15}N-^{1}H-CPVC 3D spectrum with two extracted 1D slices.

To have site specific information about the dipolar couplings, $D_{1H\text{-}15N}$, one can either only scale up by √2 the dipolar splittings (Δ) measured on the 1D dipolar slices extracted from the 3D cube, or perform full dipolar lineshape analyses using AHT equations to determine the correct dipolar values. We have compared the two methods with numerical simulations. In Fig. **5**, **S9** and **S10**, we have presented the CPVC dipolar spectra observed for 10 different η

values, which allow for the comparison of the peak separation (Δ) and the actual D/√2 value. One observes that for small asymmetry parameters, η < 0.2, D/√2 and Δ are identical within 5%, which means that it is possible to use the Δ value to calculate D instead of a full simulation of dipolar spectra. For larger asymmetry values, Δ√2 is much smaller than D, and so a global dipolar lineshape fitting is required, which necessitates the usage of a model for dynamics (Fig.**S9 and S10**). This is a very useful property of CPVC, because in the case of backbone analysis we do not predict large motions that could lead to large η values. This fact strongly decreases the time and effort needed to determine the dipolar couplings. Indeed, when the S/N ratio is low or when several species overlap in the dipolar 1D slice, it is much easier to determine directly the Δ values than to simulate the D ones. We have also compared in Table S2 the results obtained from direct splitting measurements (scaled up by 1.41) and from the lineshape fitting across the GB-1_{Cu} backbone. Both values are in good agreement, except that the D values determined from lineshape fitting are slightly higher than those obtained from direct splitting measurements. When η ≥ 0.2, which can be the case of side-chains aromatics, it is possible to use the Δ value for a first qualitative analysis of the dynamics process. This observation is consistent with our previous simulations,[73] where several full lineshapes were compared with various D and η values.

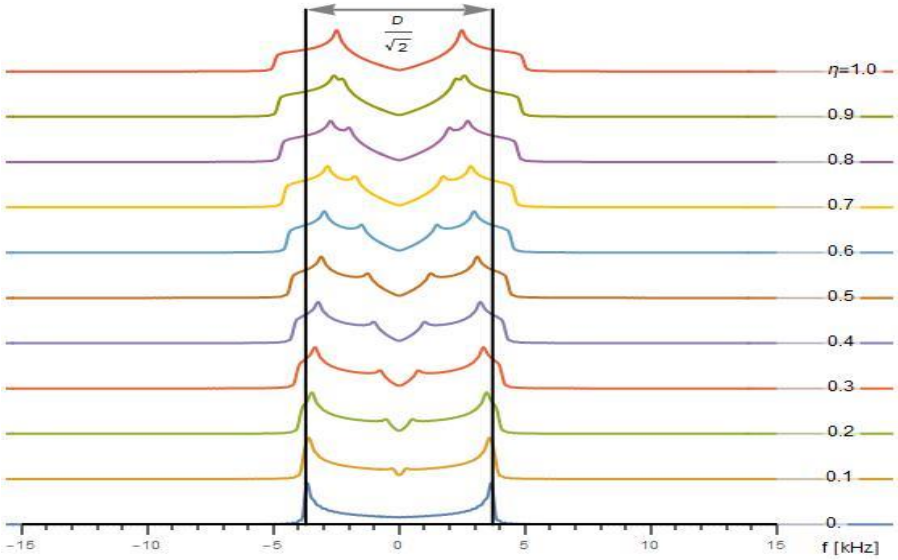

Figure 5. Dipolar doublets calculated for D = 10.5 kHz and 10 various η values. In the simulations we used the equations published in ref [77**]** and presented in the ESI. For different D values, it must be noted that the dipolar lineshapes are only scaled by the D value (Fig.**S10**).

One of the major drawbacks of the 3D inverse-detected ^{1}H-^{15}N-^{1}H CPVC approach is the impossibility to determine the D value when δ_{1H} and δ_{15N} are very close for two or more residues. In such case, a large overlap in the 1D dipolar slice occurs, and the true D or Δ values are difficult to extract, even in the case of the small GB-1_{Cu} protein. As an example, this overlapping occurs for Gly-38 and Gly-41, for which δ_{1H} and δ_{15N} values are almost the same, as observable in a strip plot from hCANH (Figure 2). In such a case, other edition methods of the dipolar coupling must be considered. One possibility is to use Cα as an editing nucleus instead of ^{15}N. To that purpose, in this work, we have developed a new 3D hCA(N)H-CPVC method, as an extension of the existing Pintacuda's sequence (Fig.6).[36]

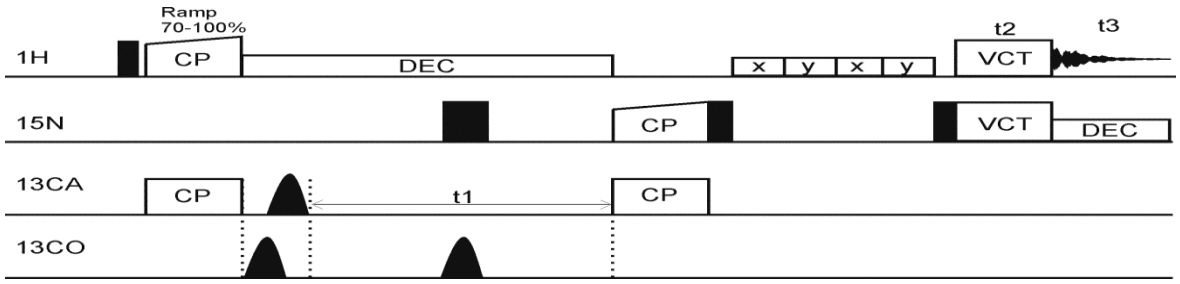

Figure 6. 3D hCA(N)H-CPVC sequence. Most parameters (phase cycling, delays, etc) are the same as in Pintacuda's paper.[36] The only differences are that (i) there is no δ_{15N} evolution, and (ii) the last $^{15}N \rightarrow {}^{1}H$ CP transfer uses constant rf amplitudes for CPVC.

It is obvious that a CO editing is also possible, giving the hCO(N)H-CPVC method, but Cα species have a higher chemical shift range than CO. More generally, in the case of very high overlapping spectra, this approach could by further extended to a 4D sequence with three chemical shift axes (δ_{1H}, δ_{15N}, $\delta_{13C\alpha}$) and one dipolar dimension ($D_{1H\text{-}15N}$). In Fig.**7** we present the 1D dipolar slices extracted for Gly-38 and Gly-41 from two 3D experiments, ^{1}H-^{15}N-^{1}H- and hCA(N)H-CPVC.

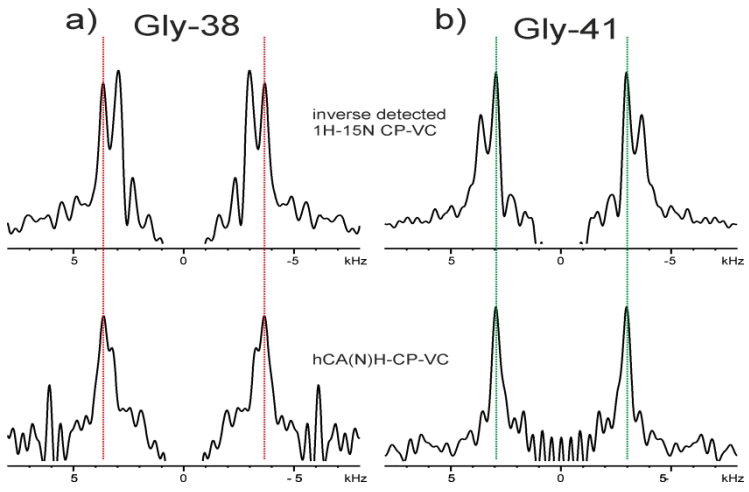

Fig.7. 1D dipolar slices from ^{1}H-^{15}N-^{1}H- and hCA(N)H-CPVC extracted for a) Gly-38 and b) Gly-41.

The ^{1}H-^{15}N-^{1}H CPVC signals of the two residues present two well defined maxima (Fig.**7** top), but it is not easy to attribute them to Gly-38 or to Gly-41. The same problem probably exists in the case of relaxation measurements with ^{1}H/^{15}N editing. In contrast, hCA(N)H-CPVC experiment leads to an unambiguous determination of the two dipolar coupling values for both Gly-38 and Gly-41 (Fig.**7** bottom). The chemical shift differences for ^{1}Hα, ^{15}N and ^{13}Cα of these two residues are equal to 0.03, 0.2 and 1.67 ppm (18, 12 and 250 Hz), respectively. These differences are very small for ^{1}Hα and ^{15}N, hence leading to the dipolar doublets with similar peak amplitudes observed with ^{1}H-^{15}N-^{1}H CPVC on the first line. For ^{13}Cα this shift difference is much higher, allowing a clear separation of the two contributions in Fig.**7** bottom. Signal overlap for these residues is also clearly visible in the case of hNH 2D spectra (Fig.**S11**), whereas resolved peaks are observed in the cases of 2D hNCO (Fig.**S13**) and especially hNCa (Fig.**S12**).

Theoretically, ^{1}H-^{15}N-^{1}H and hCA(N)H CPVC experiments should provide the same dipolar values. However, small non-systematic differences between the values obtained from these two experiments exist in both cases of direct measurements of Δ and numerical fitting of D and η values. On the other hand, in most cases these differences are smaller than the digital resolution, defined as SW/number of FID points, here 400 Hz (30 kHz/75), and they can be related to the limited resolution and different S/N ratios in the two experiments. Therefore, in the following part, whenever it is possible, we use the average value from the two experiments. The dipolar values from these two experiments, obtained from the Δ values or by lineshape analyses, are presented in Table **S2**. Finally, it should also be noted that the relaxation measurements using our triple resonance editing, with δ_{13C} instead of δ_{15N}, should be possible and very useful in a full detailed analysis of protein dynamics.

One of the best and simplest way to perform a dipolar coupling analysis across the backbone chain is to determine the so-called dipolar order parameter. This simple factor is defined as $S^2_{DD,i} = (D_i/D_{ref})^2$, where D_i is the observed dipolar coupling for *i*-th residue, and D_{ref} is a reference value calculated for some reference rigid system with known distance between interacting spins. It should be noted that for such analysis it is necessary to assume that the distances between interacting spins are constant over the backbone. Otherwise, a modification of $S^2_{DD,i}$ could mean a change of either D_i or the reference distance (D_{ref}). Fortunately, in the case of directly bonded H-N nuclei this assumption is generally true in the

protein backbone. When $S^2_{DD,i}$ is equal or close to 1 this means that *i*-th residue is rigid or has few motions. A much lower value of this parameter means that the analyzed residue exhibits intrinsic motions. In the case of GB-1_{Cu}, only a few residues have a $S^2_{DD,i}$ value much lower than 1 (Fig.**8**), namely: Lys-10, Thr-11, Leu-12, Thr-17, Glu-19, Asp-40 and Gly-41. Except for residue Thr-17, all of them are localized in the unstructured loop and it is easy to understand that such residues exhibit much higher motions than residues located in the α-helices or β-sheets.

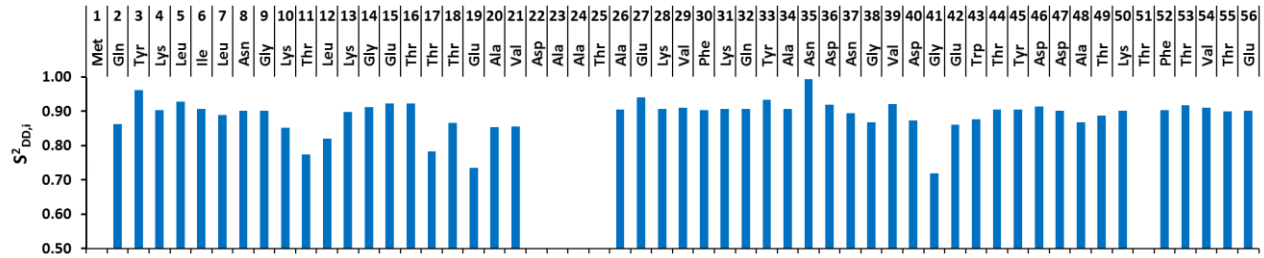

Figure 8. Dipolar ^{1}H-^{15}N order parameters defined as $S^2_{DD,i} = (D_i/D_{ref})^2$ across the GB-1_{Cu} chain. The reference value (D_{ref} = 11.35 kHz) corresponds to a rigid ^{1}H-^{15}N spin system with bond length of 1.02 Å. The average order parameter is $\langle S^2 \rangle = 0.89$.

In the 'structure calculations section' in ESI employing the CS Rosetta method, we show the higher order structure and the site-specific assignment for each individual amino acid in the GB-1_{Cu} sequence. As previously revealed, a β-hairpin is formed, stabilized by residues Trp43, Tyr45, and Phe52. Residue contacts between residue Phe30 in an α-helix and the β-hairpin strengthen the nucleation of the β-sheet starting from residues Leu5 and Phe52. The last nucleation residue, Tyr3, assists in forming the central part of the β-sheet, resulting in a globular protein. Analyzing the structure in terms of molecular dynamics, we can conclude that in the well-organized fragment of protein with strong hydrogen bonding and insufficient voids for molecular reorientation, the H-N backbone is rigid. Larger amplitude motions can be expected in loops joining the helixes and sheets. Fig.**10** displays in pictorial form the position of the amino acids under discussion in the structure of GB-1_{Cu}. It is apparent from these results that local molecular motions are strongly correlated with higher order structure of the protein. Our data are in good agreement with results published by Lewandowski and coworkers for a GB-1 sample without paramagnetic doping.[56,69] Authors employing relaxation experiments have proved that straightforward correlation between secondary structure and molecular dynamics of protein exists. We have also a good agreement with the MD simulations and the very detailed relaxation studies in solution and solid states provided by Mollica.[81] In this article, the average order parameters, $\langle S^2 \rangle \approx 0.9$, is in good agreement with

our data. For the most mobile residue (Gly41), the authors provide a value of $S^2 \approx 0.6$, whereas we find 0.72 for this residue, which can be still considered as a good agreement. The behaviors of Lys10 and Thr11 are also in good agreement between our and Mollica's data and $S^2 \approx 0.8$ in both cases. Our approach complements these studies and offers a simpler methodology.

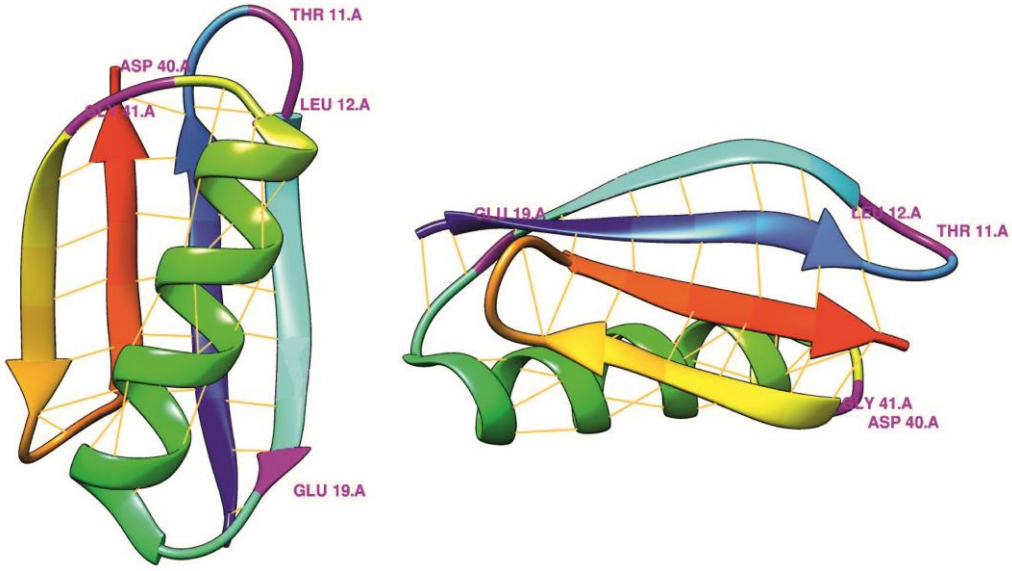

Fig.10. Model of GB-1_{Cu} obtained by means of CS Rosetta with labeled amino acids in loops joining helixes and sheets. Solid lines (orange) represent hydrogen bondings.

CONCLUSIONS

In this work, we report two new CPVC pulse sequences with ^1H detection, ^1H-^{15}N-^1H and hCA(N)H, to measure the dynamics of **H-N** vectors. Both 3D methods are applicable in proteins and other complex structures. The hCA(N)H CPVC experiment utilizes Cα instead of ^{15}N edition, which is very useful in the case of large signal overlap in the ^1H and ^{15}N dimensions. These two experiments are complementary and their simultaneous use provides much more information than the classical approaches with only $^1H/^{15}N$ chemical shift editions. They have a good sensitivity due do proton detection and they may be an alternative to relaxation measurements. It should be noted that dipolar coupling analyses are simpler to analyze, at least in a semi-quantitative way, than relaxation data. These dipolar methods are also very promising in the case of proteins with paramagnetic doping, because short relaxation delays can then be used to speed up measurements. We have demonstrated the utility of this method on a small GB-1 protein doped with $Na_2CuEDTA$. Moreover, for the first time to the best of our knowledge, we have presented ^1H, ^{15}N, CA, CB and CO

assignments of such samples, and we have compared our results with those previously published for the same protein without paramagnetic doping. Based on this chemical shift data we have determined the structure of this labeled protein, which is in good agreement with those previously reported without doping.

AUTHOR INFORMATION

Corresponding Authors

Piotr Paluch

email: ppaluch@cbmm.lodz.pl or piotr.paluch@gmail.com

Marek J. Potrzebowski

email: marekpot@cbmm.lodz.pl

§ Present Address

Univ. Lille, UMR 8181, UCCS: Unit of Catalysis and Chemistry of Solids, F-59000 Lille, France

Notes

The authors declare no competing financial interests.

ACKNOWLEDGMENTS

The authors are grateful to the Polish National Science Centre (NCN) for financial support under Grant No. UMO-2014/13/B/ST4/03050. The computational resources were partially provided by the Polish Infrastructure for Supporting Computational Science in the European Research Space (PL-GRID). Chevreul Institute (FR 2638), Ministère de l'Enseignement Supérieur et de la Recherche, Région Hauts-de-France and FEDER are acknowledged for supporting and funding partially this work. Financial support from the TGIR-RMN-THC FR 3050 CNRS for conducting the research is gratefully acknowledged. Authors also acknowledge contract CEFIPRA n°85208-E, PRC CNRS-NSFC, ANR-14-CE07-0009-01 and ANR-17-ERC2-0022 (EOS).

RERERENCES

(1) Krushelnitsky, A.; Reichert, D.; Saalwächter K. Solid-state NMR approaches to internal dynamics of proteins: from picoseconds to microseconds and seconds. *Acc. Chem. Res.* **2013,** *46*, 2028–2036.

(2) Torchia, D. A. Dynamics of biomolecules from picoseconds to seconds at atomic resolution. *J. Magn. Reson*. **2011**, *212*, 1–10.

(3) Ding, B.; Hilaire, M. R.; Gai, F. Infrared and fluorescence assessment of protein dynamics: from folding to function. *J. Phys. Chem. B* **2016**, *120*, 5103–5113.

(4) Tndo, T.; Uchihashi, T.; Kodera, N. High-speed AFM and applications to biomolecular systems, *Annu. Rev. Biophys.* **2013,** *42*, 393–414.

(5) Capitanio, M.; Pavone, F. S. Interrogating biology with force: Single molecule high-resolution measurements with optical tweezers. *Biophys. J.* **2013**, *105*, 1293**–**1303.

(6) Kleckner, I. R.; Foster, M. P. An introduction to NMR-based approaches for measuring protein dynamics. *Biochim. Biophys. Acta* **2011,** *1814*, 942–968.

(7) Zaccai, G. Neutron scattering perspectives for protein dynamics. *J. Non-Cryst. Solids* **2011,** *357*, 615–621.

(8) Adcock, S. A.; Mc Cammon, J. A. Molecular dynamics: Survey of methods for simulating the activity of proteins. *Chem. Rev.* **2006,** *106*, 1589–1615.

(9) Jaremko, Ł.; Jaremko, M.; Ejchart, A.; Nowakowski, M. Fast evaluation of protein dynamics from deficient ^{15}N relaxation data. *J. Biomol. NMR* **2018**, 1–10.

(10)Charlier C.; Cousin S.F.; Ferrage F. Protein dynamics from nuclear magnetic Relaxation Chem.Soc.Rev. **2016**, *45*, 2410-2422

(11) Ma P.; Haller J. D.; Zajakala J.; Macek P.;Sivertsen A.C.; Willbold D.; Boisbouvier J.; Schanda P. Probing transient conformational states of proteins by solid-state R(1ρ) relaxation-dispersion NMR spectroscopy**.** Angew. Chem. Int. Ed. **2014**, *53*, 4312-4317.

(12) Lewandowski J. R.; Sass H. J.; Grzesiek S.; Blackledge M.; Emsley L. Site-specific measurement of slow motions in proteins *J. Am. Chem. Soc.* 2011, **133**, 16762-16765.

(13) Tollinger M.; Sivertsen A. C.; Meier B. H.; Ernst M.; Schanda P. Site-Resolved Measurement of Microsecond-to-Millisecond Conformational-Exchange Processes in Proteins by Solid-State NMR Spectroscop J. Am.Chem. Soc. **2012**, *134*, 14800-14807

(14) Charlier C.; Khan S. N.; Marquardsen T.; Pelupessy P.; Reiss V.; Sakellariou D.; Bodenhausen G.; Engelke F.; Ferrage F. Nanosecond Time Scale Motions in Proteins Revealed by High-Resolution NMR Relaxometry J. Am. Chem. Soc. **2013**, *135*, 18665-18672.

(15) Kuwata, K.; Matumoto, T.; Cheng, H.; Nagayama, K.; James, T. L.; Roder, H. NMR-detected hydrogen exchange and molecular dynamics simulations provide structural insight into fibril formation of prion protein fragment. Proc. Natl. Acad. Sci. U. S. A.**2003,** *100*, 14790–14795.

(16) Hou, G.; Lu, X.; Vega, A. J.; Polenova, T. Accurate measurement of heteronuclear dipolar couplings by phase-alternating R-symmetry (PARS) sequences in magic angle spinning NMR spectroscopy. *J. Chem. Phys.* **2014,** *141*, 104202.

(17) Hou, G.; Byeon, I-J. L.; Ahn, J.; Gronenborn, A. M.; Polenova, T. $^{1}H–^{13}C/^{1}H–^{15}N$ hetero-nuclear dipolar recoupling by R-symmetry sequences under fast magic angle spinning for dynamics analysis of biological and organic solids. *J. Am. Chem. Soc*. **2011,** *133*, 18646–18655.

(18) Gullion, T.; Schaefer J. Rotational-Echo Double-Resonance NMR. *J. Magn. Reson.* **1989**, *81*, 196-299

(19) Schanda P.; Meier B.H.; Ernst M. Quantitative Analysis of Protein Backbone Dynamics in Microcrystalline Ubiquitin by Solid-State NMR Spectroscopy. Local Structure and Relaxation in Solid-State NMR: Accurate Measurement of Amide N−H Bond Lengths and H−N−H Bond Angles. *J. Am. Chem. Soc*. **2010** *132*, 15957-15967.

(20) Hohwy, M.; Jaroniec, C. P.; Reif, B.; Rienstra, C. M.; Griffin, R. G. *J. Am. Chem. Soc.* **2000**, *122*, 3218– 3219

(21) Helmus J.J.; Surewicz K.; Surewicz W.K.; Jaroniec C.P. Conformational Flexibility of Y145 Stop Human Prion Protein Amyloid Fibrils Probed by Solid-State Nuclear Magnetic Resonance Spectroscopy *J. Am. Chem. Soc.* **2010** *132*, 2393-2403.

(22) Chevelkov V.; Fink U.; Reif B. Accurate Determination of Order Parameters from ^{1}H, ^{15}N Dipolar Couplings in MAS Solid-State NMR Experiments *J. Am. Chem. Soc*. **2009** *131*, 14018-14022.

(23) Haller J.D.; Schanda P. Amplitudes and time scales of picosecond-to-microsecond motion in proteins studied by solid-state NMR: a critical evaluation of experimental approaches and application to crystalline ubiquitin *J.Biomol.NMR* **2013**,*57*,263-280

(24) Hou, G.; Byeon I-J. L.; Ahn, J.; Gronenborn, A. M.; Polenova, T. Recoupling of chemical shift anisotropy by R-symmetry sequences in magic angle spinning NMR spectroscopy. *J. Chem. Phys*. **2012,** *137*, 134201.

(25) Wylie B.J.; Franks W.T.; Graesser D.T.; Rienstra C.M. Site-Specific 13C Chemical Shift Anisotropy Measurements in a Uniformly 15N,13C-Labeled Microcrystalline Protein by 3D Magic-Angle Spinning NMR Spectroscopy *J. Am. Chem. Soc*. **2005,** *127*, 11946-11947.

(26) Chevelkov V.; Fink U.; Reif B. Quantitative analysis of backbone motion in proteins using MAS solid-state NMR spectroscopy *J.Biomol. NMR* **2009**, *45*, 197-206

(27) Levitt, M. H. Symmetry-Based Pulse Sequences in Magic-Angle Spinning Solid-State NMR. *Encyclopedia of Nuclear Magnetic Resonance Volume* 9, 165-196;

(28) Kristiansen, P. E.; Carravetta, M.; van Beek, J. D; Lai, W. C.; Levitt, M. H. Theory and applications of supercycled symmetry-based recoupling sequences in solid-state nuclear magnetic resonance. *J. Chem. Phys*. **2006,** *124*, 234510.

(29) Ge, Y.; Hung, I.; Liu, X.; Liu, M.; Gan, Z.; Li C. Measurement of amide proton chemical shift anisotropy in perdeuterated proteins using CSA amplification. *J. Magn. Reson.* **2017,** *284*, 33–38.

(30) Paluch, P.; Pawlak, T.; Amoureux, J-P.; Potrzebowski, M. J. Simple and accurate determination of H-X distances under ultra-fast MAS NMR. *J. Magn. Reson*. **2013,** *233*, 56–63.

(31) Nishiyama, Y. Fast magic-angle sample spinning solid-state NMR at 60–100 kHz for natural abundance samples. *Solid State Nucl. Magn. Reson.* **2016,** *78*, 24–36.

(32) Wickramasinghe, A.; Wang, S.; Matsuda, I.; Nishiyama, Y.; Nemoto, T.; Endo Y.; Ishii Y. Evolution of CPMAS under fast magic-angle-spinning at 100 kHz and beyond. *Solid State Nucl. Magn. Reson*. **2015,** *72*, 9–16.

(33) Linser R.; Chevelkov V.; Diehl A.; Reif B. Sensitivity enhancement using paramagnetic relaxation in MAS solid-state NMR of perdeuterated proteins. *J. Magn. Reson.* **2007** *189*, 209–216

(34) Cala-De Paepe, D.; Stanek, J.; Jaudzems, K.; Tars, K.; Andreas, L. B.; Pintacuda, G. Is protein deuteration beneficial for proton detected solid-state NMR at and above 100 kHz magic-angle spinning? *Solid State Nucl. Magn. Reson.* **2017,** *87*, 126–136.

(35) Wang, S.; Parthasarathy, S.; Xiao, Y.; Nishiyama, Y.; Long, F.; Matsuda, I.; Endo, Y.; Nemoto, T.; Yamauchi, K.; Asakura, T. et al. Nano-mole scale sequential signal assignment by 1H-detected protein solid-state NMR. *Chem. Commun.* **2015,** *51*, 15055–15058.

(36) Barbet-Massin, E.; Pell, A. J.; Retel, J. S.; Andreas, L. B.; Jaudzems, K.; Franks, W. T.; Nieuwkoop, A. J.; Hiller, M.; Higman, V.; Guerry, P. et al. Rapid proton-detected NMR assignment for proteins with fast magic angle spinning. *J. Am. Chem. Soc*. **2014,** *136*, 12489–12497.

(37) Marchetti, A.; Jehle, S.; Felletti, M.; Knight, M. J.; Wang, Y.; Xu, Z-Q.; Park, A. Y.; Otting, G.; Lesage, A.; Emsley. et al. Backbone assignment of fully protonated solid proteins by ^{1}H detection and ultrafast magic-angle-spinning NMR spectroscopy. *Angew. Chem., Int. Ed.* **2012,** *51*, 10756–10759.

(38) Helmus, J. J.; Jaroniec, C. P. Nmrglue: An open source Python package for the analysis of multidimensional NMR data. *J. Biomol. NMR* **2013,** *55*, 355–367.

(39) https://www.nmrglue.com/

(40) Franks, W. T.; Zhou, D. H.; Wylie, B. J.; Money, B. G.; Graesser, D. T.; Frericks, H. L.; Sahota, G.; Rienstra, C. M. Magic-angle spinning solid-state NMR spectroscopy of the β1 immunoglobulin binding domain of protein G (GB1): ^{15}N and ^{13}C Chemical shift assignments and conformational analysis. *J. Am. Chem. Soc.* **2005,** *127*, 12291–12305.

(41) Franks, W. T.; Kloepper, K. D.; Wylie, B. J.; Rienstra, C. M. Four-dimensional heteronuclear correlation experiments for chemical shift assignment of solid proteins. *J Biomol. NMR* **2007,** *39*, 107–131.

(42) Zhou, D. H.; Shah, G.; Cormos, M.; Mullen, C.; Sandoz D.; Rienstra, C. M. Proton-detected solid-state NMR spectroscopy of fully protonated proteins at 40 kHz magic-angle spinning. *J. Am. Chem. Soc.* **2007,** *129*, 11791–11801.

(43) Zhou, D. H.; Shea, J. J.; Nieuwkoop, A. J.; Franks, W. T.; Wylie, B. J.; Mullen, C.; Sandoz, D.; Rienstra C. M. Solid-state protein structure determination with proton-detected triple resonance 3D magic-angle spinning NMR spectroscopy. *Angew. Chem., Int. Ed.* **2007,** *46*, 8380–8383.

(44) Fraga, H.; Arnaud, C. A.; Gauto, D. F.; Audin, M.; Kurauskas, V.; Macek, P.; Krichel, C.; Guan, J-Y.; Boisbouvier, J.; Sprangers, R. et al. Solid-state NMR H–N–(C)–H and H–N–C–C 3D/4D correlation experiments for resonance assignment of large proteins. *ChemPhysChem* **2017,** *18*, 2697–2703.

(45) Agarwal, V.; Penzel, S.; Szekely, K.; Cadalbert, R.; Testori, E.; Oss, A.; Past, J.; Samoson, A.; Ernst, M.; Böckmann, A.; Meier B.H. De novo 3D structure determination from sub-milligram protein samples by solid-state 100 kHz MAS NMR spectroscopy. *Angew. Chem., Int. Ed*. **2014,** *53*, 12253–12256.

(46) Penzel, S.; Smith, A. A.; Agarwal, V.; Hunkeler, A.; Org, M-L.; Samoson, A.; Böckmann, A.; Ernst, M.; Meier, B. H. Protein resonance assignment at MAS frequencies approaching 100 kHz: a quantitative comparison of J-coupling and dipolar-coupling-based transfer methods. *J. Biomol. NMR* **2015,** *63*, 165–186.

(47) Schmidt, H. L.; Sperling, L. J.; Gao, Y. G.; Wylie, B. J.; Boettcher, J. M.; Wilson, S. R.; Rienstra, C. M. Crystal polymorphism of protein GB1 examined by solid-state NMR spectroscopy and X-ray diffraction. *Phys. Chem. B* **2007,** *111*, 14362–14369.

(48) Ma, P.; Xue, Y.; Coquelle, N.; Haller, J.D.; Yuwen, T.; Ayala, I.; Mikhailovskii, O.; Willbold, D.; Colletier, J.; Skrynnikov, N.R.; et al. Observing the overall rocking motion of a protein in a crystal. Nat. Commun. **2015**, *6*, 8361

(49) Cavanagh, J.; Fairbrother, W. J.; Palmer III, A. G.; Rance, M.; Skelton, N. J. *Protein NMR Spectroscopy: Principles and Practice* (Academic Press)

(50) Wickramasinghe, N. P.; Parthasarathy, S.; Jones, C. R.; Bhardwaj, C.; Long, F.; Kotecha, M.; Mehboob, S.; Fung, L-W. M.; Past, J., Samoson, A.; Ishii, Y. Nanomole-scale Protein solid-state NMR by breaking intrinsic ^{1}H-T_1 boundaries. *Nat. Methods* **2009,** *6*, 215–218.

(51) Ishii, Y.; Wickramasinghe, A.; Matsuda, I.; Endo, Y.; Ishii, Y.; Nishiyama, Y.; Nemoto, T.; Kamihara, T. Progress in proton-detected solid-state NMR (SSNMR): Super-fast 2D SSNMR collection for nano-mole-scale proteins. *J. Magn. Reson.* **2018,** *286*, 99–109.

(52) Bertini, I.; Luchinat, C.; Parigi, G. Paramagnetic constraints: an aid for quick solution structure determination of paramagnetic metalloproteins. *Concepts Magn. Reson.* **2002**, *14*, 259–286.

(53) Bax, A. Triple resonance three-dimensional protein NMR: Before it became a black box, *J. Magn. Reson.* **2011,** *213*, 442–445;

(54) Sattler, M.; Schleucher, J.; Griesinger, C. Heteronuclear multidimensional NMR experiments for the structure determination of proteins in solution employing pulsed field gradients, *Prog. Nucl. Magn. Reson. Spectrosc.***1999,** *34*, 93–158.

(55) Chen L.; Kaiser J.M.; Polenova T.; Yang J.; Rienstra C.M.; Mueller L.J. Backbone Assignments in Solid-State Proteins Using J-Based 3D Heteronuclear Correlation Spectroscopy. *J. Am. Chem. Soc.* **2007,** *129*,1-650-10651

(56) Lamley, J. M.; Lougher, M. J.; Sass, H. J.; Rogowski, M.; Grzesiek, S.; Lewandowski J. R. Unravelling the complexity of protein backbone dynamics with combined ^{13}C and ^{15}N solid-state NMR relaxation measurements. *Phys. Chem. Chem. Phys.* **2015,** *17*, 21997–22008.

(57) Schanda P.; Ernst M. Studying dynamics by magic-angle spinning solid-state NMR spectroscopy: Principles and applications to biomolecules. Prog,Nuc.Magn.Reson. **2016**, *96*, 1-46

(58) Lamley J.M.; Lewandowski J.R. Relaxation-Based Magic-Angle Spinning NMR Approaches for Studying Protein Dynamics, *eMagRes* **2016**, *5*, 1423–1434

(59) Pawlak, T.; Trzeciak-Karlikowska, K.; Czernek, J.; Ciesielski, W.; Potrzebowski, M. J. Computed and experimental chemical shift parameters for rigid and flexible YAF peptides in the solid state. *J. Phys. Chem. B* **2012**, *116*, 1974–1983.

(60) Dvinskikh, S. V.; Zimmermann, H.; Maliniak, A.; Sandström, D.; Measurements of motionally averaged heteronuclear dipolar couplings in MAS NMR using R-type recoupling. *J. Magn. Reson.* **2005,** *175*, 163–169.

(61) Krushelnitsky, A.; Reichert, D.; Hempel, G.; Fedotov, V.; Schneider, H.; Yagodina L.; Schulga, A. Superslow backbone protein dynamics as studied by 1D solid-state MAS exchange NMR spectroscopy. *J. Magn. Reson.* **1999,** *138*, 244–255.

(62) Krushelnitsky, A.; Reichert, D.; Saalwachter K. Solid-State NMR Approaches to Internal Dynamics of Proteins: From Picoseconds to Microseconds and Seconds. Acc.Chem.Res. **2013**,*46*,2028-2036

(63) Piślewski, N.; Tritt-Goc, J.; Bilejewski, M.; Rachocki, A.; Ratajczyk, T.; Szymanski S. Spin-lattice relaxation study of the methyl proton dynamics in solid 9,10-dimethyltriptycene (DMT). *J. Magn. Reson.* **2009,** *35*, 194–200.

(64) Leisen, J.; Schmidt-Rohr K.; Spiess H. W. Multidimensional ^{2}H NMR studies of the non-exponential chain relaxation of polystyrene above the glass transition. *J. Non-Cryst. Solids,* **1994**, *172-174*, 737–750.

(65) Schanda, P.; Ernst, M. Studying dynamics by magic-angle spinning solid-state NMR spectroscopy: Principles and applications to biomolecules. *Prog. Nucl. Magn. Reson. Spectrosc.* **2016,** *96*, 1–46.

(66) Lipari, G.; Szabo, A. Model-free approach to the interpretation of nuclear magnetic-resonance relaxation in macromolecules: 1. Theory and range of validity. *J. Am. Chem. Soc.* **1982,** *104*, 4546–4559;

(67) Jaremko, Ł.; Jaremko, M.; Nowakowski, M.; Ejchart, A. The quest for simplicity: Remarks on the free-approach models. *J. Phys. Chem. B* **2015,** *119*, 11978–11987.

(68) Jaroniec C.J. Structural studies of proteins by paramagnetic solid-state NMR Spectroscopy. *J. Magn. Reson.* **2015,** 253, 50–59.

(69) Lamley, J. M.; Oster, C.; Stevens, R. A.; Lewandowski, J. R. Intermolecular interactions and protein dynamics by solid-state NMR spectroscopy. *Angew. Chem., Int. Ed.* **2015,** *54*, 15374–15378.

(70) Schanda P.; Huber M.; Boisbouvier J.; Meier B.H.; Ernst M. Solid-State NMR Measurements of Asymmetric Dipolar Couplings Provide Insight into Protein Side-Chain Motion. *Angew. Chem., Int. Ed.* **2011**, *50*,11005-11009

(71) Paluch, P.; Trébosc, J.; Amoureux, J-P.; Potrzebowski, M. J. ^{1}H-^{31}P CPVC NMR method under Very Fast Magic Angle Spinning for analysis of dipolar interactions and dynamics processes in the crystalline phosphonium tetrafluoroborate salts. *Solid State Nucl. Magn. Reson.* **2017**, *87*, 96–103.

(72) Dudek, M. K.; Pawlak, T.; Paluch, P.; Jeziorna, A.; Potrzebowski, M. J. A multi-technique experimental and computational approach to study the dehydration processes in the crystals of endomorphin opioid peptide derivative. *Cryst. Growth Des.* **2016,** *16*, 5312–5322.

(73) Paluch, P.; Trébosc, J.; Nishiyama, Y.; Potrzebowski, M. J.; Malon, M.; Amoureux, J-P. Theoretical study of CPVC: a simple, robust and accurate MAS NMR method for analysis of dipolar C-H interactions under rotation speeds faster than ca. 60 kHz. *J. Magn. Reson.* **2015,** 252, 67–77.

(74) Nishiyama, Y.; Malon, M.; Potrzebowski, M. J.; Paluch, P.; Amoureux, J-P. Accurate NMR determination of C–H or N–H distances for unlabelled molecules. *Solid State Nucl. Magn. Reson.* **2016,** *73*, 5–21.

(75) Rajput, L.; Banik, M.; Yarava, J. R.; Joseph, S.; Pandey, M. K.; Nishiyama Y.; Desirajua G. R. Exploring the salt-cocrystal continuum with solid-state NMR using natural-abundance samples: implications for crystal engineering. *IUCrJ,* **2017,** *4*, 466–475.

(76) Park, S. H.; Yang, C.; Opella, S. J.; Mueller, L. J. Resolution and measurement of hetero-nuclear dipolar couplings of a non-crystalline protein immobilized in a biological supra-molecular assembly by proton-detected MAS solid-state NMR spectroscopy. *J. Magn. Reson.* **2013,** *237*, 164–168.

(77) Paluch, P.; Pawlak, T.; Jeziorna, A.; Trébosc J.; Hou, G.; Vega, A. J.; Amoureux, J-P.; Dracinsky, M.; Polenova, T.; Potrzebowski, M. J. Analysis of local molecular motions of aromatic side chains in proteins by 2D and 3D fast MAS NMR spectroscopy and quantum mechanical calculations. *Phys. Chem. Chem. Phys.* **2015,** *17*, 28789–28801.

(78) Wiench, J. W.; Bronnimann, C. E.; Lin, V.S.-Y.; Pruski, M. Chemical shift correlation NMR spectroscopy with indirect detection in fast rotating solids: studies of organically functionalized mesoporous silicas. *J. Am.Chem. Soc.* **2007,** *129*, 12076–12077.

(79) Mao, K.; Kobayashi, T.; Wiench, J. W.; Chen, H. T.; Tsai, C. H.; Lin, V. S-Y; Pruski, M. Conformations of silica-bound (pentafluorophenyl)propyl groups determined by solid-state NMR spectroscopy and theoretical calculations. *J. Am. Chem. Soc.* **2010,** *132*, 12452–12457.

(80) Kobayashi, T.; Mao, K.; Paluch, P.; Nowak-Król, A.; Śniechowska, J.; Nishiyama, Y.; Gryko, D. T.; Potrzebowski, M. J.; Pruski, M. Study of intermolecular interactions in the corrole matrix by solid-state NMR under 100 kHz MAS and theoretical calculations. *Angew. Chem., Int. Ed.* **2013,** *52*, 14108–14111.

(81) Mollica L.; Bais M.; Lewandowski J.L.; Wylie B.J.; Sperling L.J.; Rienstra C.M.; Emsley L.; Blackledge M. Atomic-Resolution Structural Dynamics in Crystalline Proteins from NMR and Molecular Simulation J. Phys. Chem. Lett. **2012**, **3**, 3657−3662

Graphical Abstract